

See discussions, stats, and author profiles for this publication at: <https://www.researchgate.net/publication/261767560>

Chelate Effects in Glyme/Lithium Bis(trifluoromethanesulfonyl)amide Solvate Ionic Liquids. I. Stability of Solvate Cations and Correlation with Electrolyte Properties

ARTICLE in THE JOURNAL OF PHYSICAL CHEMISTRY B · APRIL 2014

Impact Factor: 3.3 · DOI: 10.1021/jp501319e · Source: PubMed

CITATIONS

17

READS

115

9 AUTHORS, INCLUDING:



Kazuhide Ueno

Yamaguchi University

69 PUBLICATIONS 1,244 CITATIONS

SEE PROFILE



Toshihiko Mandai

Chalmers University of Technology

27 PUBLICATIONS 250 CITATIONS

SEE PROFILE



Kaoru Dokko

Yokohama National University

140 PUBLICATIONS 3,021 CITATIONS

SEE PROFILE



Masayoshi Watanabe

Yokohama National University

350 PUBLICATIONS 14,344 CITATIONS

SEE PROFILE

Chelate Effects in Glyme/Lithium Bis(trifluoromethanesulfonyl)amide Solvate Ionic Liquids. I. Stability of Solvate Cations and Correlation with Electrolyte Properties

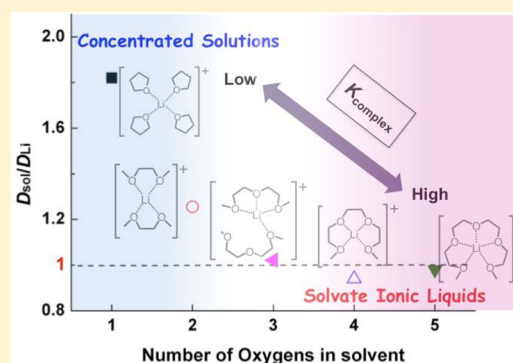
Ce Zhang,^{†,§} Kazuhide Ueno,^{†,§} Azusa Yamazaki,[†] Kazuki Yoshida,[†] Heejoon Moon,[†] Toshihiko Mandai,[†] Yasuhiro Umebayashi,[‡] Kaoru Dokko,[†] and Masayoshi Watanabe^{*,†}

[†]Department of Chemistry and Biotechnology, Yokohama National University, 79-5 Tokiwadai, Hodogaya-ku, Yokohama 240-8501, Japan

[‡]Graduate School of Science and Technology, Niigata University, 8050 Ikarashi 2no-cho, Nishi-ku, Niigata 950-2181, Japan

S Supporting Information

ABSTRACT: To develop a basic understanding of a new class of ionic liquids (ILs), “solvate” ILs, the transport properties of binary mixtures of lithium bis(trifluoromethanesulfonyl)amide (Li[TFSA]) and oligoethers (tetraglyme (G4), triglyme (G3), diglyme (G2), and monoglyme (G1)) or tetrahydrofuran (THF) were studied. The self-diffusion coefficient ratio of the solvents and Li⁺ ions ($D_{\text{sol}}/D_{\text{Li}}$) was a good metric for evaluating the stability of the complex cations consisting of Li⁺ and the solvent(s). When the molar ratio of Li⁺ ions and solvent oxygen atoms ($[\text{O}]/[\text{Li}^+]$) was adjusted to 4 or 5, $D_{\text{sol}}/D_{\text{Li}}$ always exceeded unity for THF and G1-based mixtures even at the high concentrations, indicating the presence of uncoordinating or highly exchangeable solvents. In contrast, long-lived complex cations were evidenced by a $D_{\text{sol}}/D_{\text{Li}} \sim 1$ for the longer G3 and G4. The binary mixtures studied were categorized into two different classes of liquids: concentrated solutions and solvate ILs, based on $D_{\text{sol}}/D_{\text{Li}}$. Mixtures with G2 exhibited intermediate behavior and are likely the borderline dividing the two categories. The effect of chelation on the formation of solvate ILs also strongly correlated with electrolyte properties; the solvate ILs showed improved thermal and electrochemical stability. The ionicity ($\Lambda_{\text{imp}}/\Lambda_{\text{NMR}}$) of $[\text{Li}(\text{glyme or THF})_x][\text{TFSA}]$ exhibited a maximum at an $[\text{O}]/[\text{Li}^+]$ ratio of 4 or 5.



1. INTRODUCTION

Solvate ionic liquids are a new class of room-temperature ionic liquids (ILs) in which ligand molecules, as a third species of the liquids, strongly solvate the cations and/or anions of salts to form complex ions. The criteria for the formation of solvate ILs primarily depend on the formation of stable complex salts possessing a lower melting point. The basic concept of this new subclass of ILs was reported by Angell in 1965, who regarded the hydrated calcium cation as an independent cation in hydrated molten salts of $\text{Ca}(\text{NO}_3)_2 \cdot 4\text{H}_2\text{O}$.¹ Following this discovery, Angell et al. named this category of low-melting molten complexes as solvate ILs in their latest review article.²

We have previously reported that molten complexes consisting of 1:1 equimolar mixtures of lithium bis-(trifluoromethanesulfonyl)amide (Li[TFSA]) and triglyme (G3) or tetraglyme (G4) behave like typical ILs through the formation of crown ether-like complex cations $[\text{Li}(\text{G3 or G4})]^+$, and were thus judged as representative of solvate ILs.^{3–5} The lithium solvate ILs exhibit many desirable properties as a lithium-conducting electrolyte, including high lithium transference numbers, high Li⁺ ion concentration, and improved oxidative stability,^{5,6} in addition to commonly observed features of ILs such as low vapor pressure and high

thermal stability. These characteristics allowed the successful operation of lithium ion batteries with various cathode and anode materials.^{7,8} Furthermore, the lithium solvate ILs proved to be effective electrolytes for the suppression of undesired polysulfide dissolution in lithium sulfur batteries, leading to a noteworthy discharge capacity of ca. 700 mA h g^{−1} sulfur with high Coulombic efficiency (>98%),^{9–11} even after 400 charge/discharge cycles. These extraordinary properties, such as enhanced oxidative stability,¹² and the greatly suppressed solubility of polysulfides^{13,14} have also been found in highly concentrated Li[TFSA] electrolytes in low-molecular weight organic solvents, commonly used in lithium-ion battery electrolytes.

Given that solvate ILs and “classical” concentrated electrolyte solutions are considered very similar in composition—the number of solvent molecules and ions is comparable or almost equal for both systems—the categorization of these liquids is still ambiguous. To develop a basic understanding of solvate ILs and their unique properties, more elaborate criteria to divide

Received: February 6, 2014

Revised: April 21, 2014

Published: April 21, 2014

solvate ILs from common electrolyte solutions are essential. In a previous study,¹⁵ the anion-dependent properties of equimolar molten mixtures of different lithium salts (LiX) and G3/G4, $[\text{Li}(\text{G3 or G4})_1]\text{X}$, were studied. $[\text{Li}(\text{G3 or G4})_1]\text{X}$ was classified as either a “concentrated solution” or a “solvate IL”, depending on the stability of the $[\text{Li}(\text{G3 or G4})_1]^+$ cation. There was crucial competition between Coulombic interactions (Li^+-X^-) and ion–dipole (induced dipole) interactions (Li^+-glyme) in highly concentrated $[\text{Li}(\text{G3 or G4})_1]\text{X}$, and the stable complex cations were formed only when the former interaction overwhelmed the latter, in other words combined with weakly coordinating counteranions such as $[\text{TFSA}]^-$ (lower Li^+-X^- interactions).

In coordination chemistry, the stability of complex ions is strongly dictated by the structure of ligand molecules. In this study we investigate a structurally related series of concentrated mixtures of $\text{Li}[\text{TFSA}]$ and oligoether solvents to clarify the effect of ion–dipole (or ion-induced dipole) interactions on the formation of solvate ILs. Whereas G3 and G4 possess 4 and 5 coordination sites, respectively, in each molecule to chelate the Li^+ ion, the number of oxygen atoms per molecule becomes smaller for diglyme (G2), monoglyme (G1), and tetrahydrofuran (THF). Although the enhanced stability of complex ions with multidentate ligands is well-known through the chelate effect, the studies have been generally performed in dilute solutions or in the crystalline state. The main purpose of this investigation was to study the dynamics of the chelate effect on the stability of lithium complex cations (i.e., the formation of solvate ILs) in extremely concentrated liquid states. The physicochemical properties of the concentrated mixtures were explored at constant $[\text{O}]/[\text{Li}^+]$ ratios of 4 or 5 and compared with those for the previously reported $[\text{Li}(\text{G3 or G4})_1][\text{TFSA}]$. The study demonstrates that the stabilities of complex cations are clearly reflected in their thermal and electrochemical properties, as well as the transport properties of these concentrated electrolytes.¹⁶

2. EXPERIMENTAL SECTION

Materials. Glymes with the chemical structure of $\text{CH}_3-\text{O}-(\text{CH}_2-\text{CH}_2-\text{O})_n-\text{CH}_3$ ($n = 1-5$) are abbreviated as G1–G5, respectively. Monoglyme (G1) and diglyme (G2) were purchased from Kishida Chemical (battery grade reagents), and super-dehydrated tetrahydrofuran ($[\text{H}_2\text{O}] < 10$ ppm) was purchased from Wako Pure Chemical. Triglyme (G3) and tetraglyme (G4) were obtained from Tokyo Chemical Industry and were distilled under reduced pressure over sodium metal. Purified pentaglyme (G5) was kindly supplied by Nippon Nyukazai and used as received. $\text{Li}[\text{TFSA}]$ was obtained from Morita Chemical Industries and dried under vacuum at 120 °C before use. The solutions were prepared by mixing the solvent and $\text{Li}[\text{TFSA}]$ in different molar ratios and stirring overnight at room temperature to obtain homogeneous liquids. The mixtures were prepared, stored, and handled in an argon-filled glovebox (VAC, $[\text{H}_2\text{O}] < 1$ ppm).

Measurements. Ionic conductivities of the electrolyte solutions were determined by the complex impedance method using an AC impedance analyzer (Princeton Applied Research, VMP2) in a frequency range of 1–500 kHz at an amplitude of 10 mV. A conductivity cell possessing two electrodes of platinized platinum (TOA Electronics, CG-511B; cell constant = approximately 1 cm^{-1}) was used for conductivity measurements. The cell constant for the conductivity measurements was determined by calibration with 0.01 M KCl standard

solution (Kanto Chemical). The cell was placed in a temperature-controlled chamber to ensure thermal equilibrium for at least 60 min. The relative uncertainty for conductivity values was <1%. The temperature dependence of viscosity and density were measured using an SVM3000 viscometer (Anton Paar). Uncertainties of density and viscosity values were $\pm 0.0005 \text{ g cm}^{-3}$ and $\pm 0.35\%$, respectively. Raman spectra were measured using a 532 nm laser RMP-300 Raman spectrometer (JASCO) at room temperature between 200 and 1700 cm^{-1} . All spectra were recorded in the liquid state. Raman spectral bands were analyzed for different concentrations with baseline correction using a JASCO spectra manager program. Thermogravimetric analysis was performed using a TG/TDA 6200 apparatus (Hitachi High-tech Science) under a nitrogen atmosphere from room temperature to 550 °C at a heating rate of $10 \text{ }^\circ\text{C min}^{-1}$. In this study, the thermal decomposition temperature (T_d) was defined as the temperature of a 5% mass loss in the thermogravimetric curves.

The oxidative electrochemical stabilities of the binary $\text{Li}[\text{TFSA}]/\text{ether}$ mixtures were studied using linear sweep voltammetry (LSV) at a scan rate of 1 mV s^{-1} in a three-electrode cell, with Li metal foil as the counter electrode, and a platinum disk (diameter 1 mm) encapsulated in a shrinkable fluorinated tube as the working electrode. The reference electrode was Li metal soaked in $1 \text{ mol dm}^{-3} \text{ Li}[\text{TFSA}]/\text{G3}$ solution, confined in a glass tube equipped with a liquid junction (Vycor glass).

Pulsed-field gradient spin echo (PGSE) NMR measurements were carried out to determine the self-diffusion coefficients of the components of the electrolyte solutions. A JEOL ECX-400 NMR spectrometer with a 9.4 T narrow-bore superconducting magnet and a pulsed-field gradient probe was used for the measurements. ^1H , ^7Li , and ^{19}F NMR spectra were recorded for the solvents, Li^+ , and $[\text{TFSA}]^-$, respectively. The self-diffusion coefficients were measured via the use of a modified Hahn spin echo-based PGSE sequence incorporating a pulsed-field gradient (PFG) in each τ period. The detailed measurement procedures for PGSE NMR are described elsewhere.¹⁷ The free diffusion echo signal attenuation E is related to the experimental parameters by the Stejskal equation with sinusoidal PFG:¹⁸

$$\ln(E) = \ln(S/S_{\delta=0}) = \frac{-\gamma^2 g^2 D \delta^2 (4\Delta - \delta)}{\pi^2} \quad (1)$$

where S is the spin echo signal intensity, δ is the duration of the field gradient with magnitude g , γ is the gyromagnetic ratio, and Δ is the interval between the two gradient pulses. The values of Δ (50 ms) and δ (1–10 ms) were set at constant value, whereas g (0–13 T/m) was varied for the diffusion measurements. All of the results were well-described by eq 1, and the standard deviations of the diffusion data were less than 5%. The PGSE NMR samples were inserted into a NMR microtube (BMS-005J, Shigemitsu) to a height of 3 mm to exclude convection. All measurements were performed at 30 °C.

3. RESULTS AND DISCUSSION

Concentration Dependence of Transport Properties.

Although our primary focus in this study concerned highly concentrated regions of the mixtures of $\text{Li}[\text{TFSA}]$ and ether solvents, we first reexamined the transport properties of mixtures ranging from dilute ($\sim 0.01 \text{ mol dm}^{-3}$) and intermediate ($\sim 0.5 \text{ mol dm}^{-3}$) to extremely concentrated

states (up to 3.7 mol dm^{-3}). Figures 1 and 2 show the isothermal ionic conductivity and viscosity of $[\text{Li}(\text{glyme or THF})_x][\text{TFSA}]$ mixtures at 30°C .

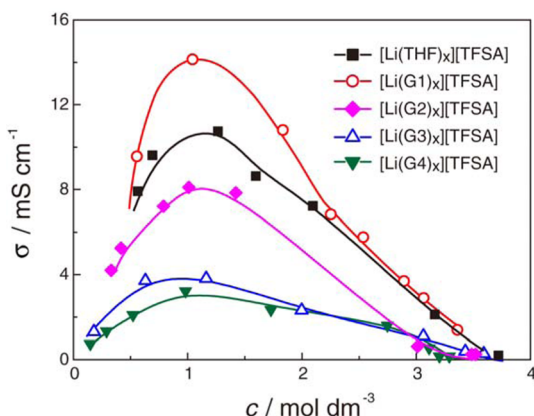


Figure 1. Concentration dependence of ionic conductivity for $[\text{Li}(\text{glyme or THF})_x][\text{TFSA}]$ mixtures at 30°C . Lines are a guide to the eye.

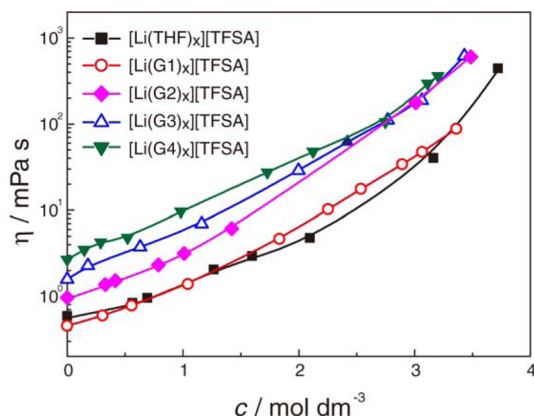


Figure 2. Concentration dependence of viscosity for $[\text{Li}(\text{glyme or THF})_x][\text{TFSA}]$ solutions at 30°C . Lines are a guide to the eye.

$[\text{Li}(\text{glyme or THF})_x][\text{TFSA}]$ mixtures at 30°C . Similar to studies reported elsewhere,^{19,20} the ionic conductivity increases as the concentration increases below 1 mol dm^{-3} , reaching a

maximum at ca. 1 mol dm^{-3} , and then decreases with further increases in the concentration. For $[\text{Li}(\text{G2})_x][\text{TFSA}]$ mixtures, limited data are shown in the concentrated regime because only a few appropriate ratios ($\text{G2/Li}[\text{TFSA}] = 1:1, 4:3, \text{ and } 4:1$) yielded liquid samples at 30°C . In the dilute regime, the conductivity increases in the order of the ether solvents $\text{G1} > \text{THF} > \text{G2} > \text{G3} > \text{G4}$ at the same concentration.

The dependency of viscosity on concentration for $[\text{Li}(\text{glyme or THF})_x][\text{TFSA}]$ is shown in Figure 2 and is compared with the reported data for $[\text{Li}(\text{G3 or G4})_x][\text{TFSA}]$.¹⁹ The viscosity is lower for the mixtures with shorter ethers (i.e., G1 and THF) at the same concentration. The lower viscosity thus accounts for the higher ionic conductivity of $[\text{Li}(\text{G1})_x][\text{TFSA}]$ compared to $[\text{Li}(\text{G3 or G4})_x][\text{TFSA}]$. As seen in Figure 1, however, the conductivity of $[\text{Li}(\text{THF})_x][\text{TFSA}]$ is lower than those for $[\text{Li}(\text{G1})_x][\text{TFSA}]$ despite the comparable viscosity for these solutions. Other factors such as the degree of dissociation or ionicity (correlation of ionic motion) may bring about differences in ionic conductivity among G1 and THF solutions (vide infra).

The self-diffusion coefficients of the solvent, Li^+ , and $[\text{TFSA}]^-$ were measured by PGSE NMR spectroscopy, and their concentration dependence is shown in the Supporting Information (Table S1). Each diffusion coefficient decreased monotonically with increasing concentration. In the concentration range of $0\text{--}2.0 \text{ mol dm}^{-3}$, the self-diffusion coefficients followed the order $D_{\text{sol}} > D_{\text{TFSA}} > D_{\text{Li}}$, which agrees well with the order of diffusion coefficients in conventional organic electrolytes, including the glymes.^{19,21,22} However, D_{Li} became greater than D_{TFSA} in highly concentrated mixtures, implying that the coordination of Li^+ ions and their ionic diffusion differs from those in dilute systems.

In a previous study, we reported that the self-diffusion coefficient ratio of Li^+ ions and solvent molecules ($D_{\text{sol}}/D_{\text{Li}}$) is an effective metric to evaluate the stability of complex cations formed between Li^+ ions and the solvents G3 and G4.¹⁵ In typical solvate ILs such as $[\text{Li}(\text{G3})_1][\text{TFSA}]$ and $[\text{Li}(\text{G4})_1][\text{TFSA}]$, the $D_{\text{sol}}/D_{\text{Li}}$ ratio became unity, indicating that Li^+ and the glyme diffuse together and is therefore a good probe for confirming the formation of the long-lived complex cations $[\text{Li}(\text{G3 or G4})_1]^+$. Indeed, the PGSE NMR measurements were performed on the time scale of $10^{-2}\text{--}10^{-3} \text{ s}$, and the resulting D is given as the averaged value of both free and coordinated

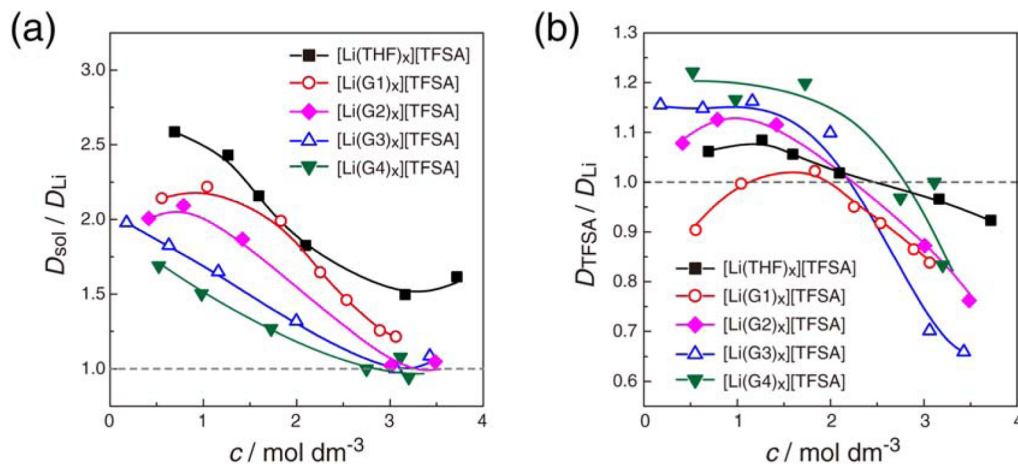


Figure 3. Concentration dependence of (a) $D_{\text{sol}}/D_{\text{Li}}$ ratio and (b) $D_{\text{TFSA}}/D_{\text{Li}}$ ratio at 30°C for $[\text{Li}(\text{glyme or THF})_x][\text{TFSA}]$ mixtures. Lines are a guide to the eye.

Table 1. Viscosity (η), Density (ρ), Molar Concentration (c), Ionic Conductivity (σ), and $D_{\text{sol}}/D_{\text{Li}}$ of the [Li(glyme or THF)_x][TFSA] Mixtures at 30 °C^a

mixtures	[O]/[Li]	η (mPa s)	ρ (g cm ⁻³)	c (mol dm ⁻³)	σ (mS cm ⁻¹)	$D_{\text{sol}}/D_{\text{Li}}$
[Li(THF) ₄][TFSA]	4	5	1.21	2.10	7.2	1.82
[Li(G1) ₂][TFSA]	4	34	1.35	2.89	3.7	1.26
[Li(G2) _{4/3}][TFSA]	4	177	1.40	3.01	0.62	1.02
[Li(G3) ₁][TFSA]	4	188	1.42	3.06	1.1	1.00
[Li(G1) _{5/2}][TFSA]	5	18	1.30	2.54	5.8	1.46
[Li(G4) ₁][TFSA]	5	106	1.40	2.75	1.6	1.00

^aSome data for [Li(G3)₁][TFSA] and [Li(G4)₁][TFSA] are obtained from ref 19.

solvent to Li⁺ ions on this time scale. Figure 3 shows the $D_{\text{sol}}/D_{\text{Li}}$ and $D_{\text{TFSA}}/D_{\text{Li}}$ ratios of [Li(glyme or THF)_x][TFSA] depending on the concentration. At lower concentrations (<2 mol dm⁻³), $D_{\text{sol}}/D_{\text{Li}}$ and $D_{\text{TFSA}}/D_{\text{Li}}$ are always greater than unity in all solvents, which is common for aprotic organic electrolyte solutions as noted above. At higher concentrations (>3 mol dm⁻³), the $D_{\text{sol}}/D_{\text{Li}}$ ratio of [Li(G1 or THF)_x][TFSA] levels off but is still greater than unity, even if the molar concentration is as high as that of the solvate ILs [Li(G3 or G4)₁][TFSA]. In sharp contrast, the $D_{\text{sol}}/D_{\text{Li}}$ ratios for [Li(G2)_x][TFSA] reach $D_{\text{sol}}/D_{\text{Li}} \sim 1$ at higher concentration, similar to the previous results for [Li(G3 or G4)_x][TFSA].¹⁹ As shown in Figure 3b, $D_{\text{TFSA}}/D_{\text{Li}}$ becomes less than unity in the concentrated regime (>2 mol dm⁻³) for all of the [Li(glyme or THF)_x][TFSA] species studied in this work, indicating that Li⁺ ions diffuse faster than [TFSA]⁻. This suggests a different conduction mechanism in highly concentrated [Li(glyme or THF)_x][TFSA]. In dilute aprotic polar solvent solutions, it is generally assumed that solvate cations [Li(glyme or THF)_x]⁺ and naked [TFSA]⁻ diffuse through continuous glyme or THF with a viscosity η , as rationalized by the Stokes–Einstein equation. In such cases, the apparent hydrodynamic radius of the solvated Li⁺ ion becomes larger than that of naked [TFSA]⁻, which is a reason for a lower Li⁺ transference number than 0.5 ($D_{\text{TFSA}}/D_{\text{Li}} > 1$). On the contrary, in highly concentrated electrolytes such as ILs, the Stokes–Einstein equation has no physicochemical meaning, even if the equation appears to hold. For instance, we have reported that, for imidazolium-based ILs, the cationic transference number becomes greater than 0.5 even when the cation is larger than the anion.²³ We observe that in highly concentrated [Li(glyme or THF)_x][TFSA] (>2 mol dm⁻³), $D_{\text{TFSA}}/D_{\text{Li}}$ becomes less than unity (cationic transference number > 0.5). The lowest value of $D_{\text{TFSA}}/D_{\text{Li}}$ for [Li(G3)₁][TFSA] (ca. 0.65) may not only be related to the compact solvate ion size but also related to anomalies in the transport properties of ILs. We experimentally observe similar phenomena that cations move faster than the anion in conventional imidazolium-based ILs and in the concentrated [Li(glyme or THF)_x][TFSA] system.

Unique diffusivity (Figure 3) observed in the highly concentrated regime may be ascribed to the fact that certain solvates are formed through complexation between the solvent molecules and the Li salts, such that there is almost no free solvent. The differences in the properties among [Li(glyme or THF)_x][TFSA] were also more obvious in these concentrated mixtures. In the next section, we will discuss the molten state behavior of such solvent–Li salt complexes in detail.

Structures of Molten Crystalline Solvates and Relevant Highly Concentrated Mixtures. Mixtures of glymes or THF and Li[TFSA] form crystalline solvates in the concentrated regime. Longer glymes such as G3, G4, and G5

tend to form a stable solvate in a 1:1 ratio with Li[TFSA].^{24–26} Crystalline [Li(G3)₁][TFSA] and [Li(G5)₁][TFSA] possess melting points of 20 and 67 °C, respectively (Supporting Information Figure S1). However, [Li(G4)₁][TFSA] did not exhibit any thermal events other than a glass transition, which may be due to crystallinity gap behavior as reported in related PEO–Li[TFSA] systems (PEO, poly(ethylene oxide)).²⁷ The mixtures with the shorter G1 and G2 involve a series of intermediate crystalline solvates. The previous reports suggested the formation of stable solvates in a 3:1 ($T_{\text{m}} = 29$ °C), 2:1 ($T_{\text{m}} = 20$ °C), and 1:1 ratio ($T_{\text{m}} = 56$ °C) for G1–Li[TFSA] mixtures; and a 2:1 ($T_{\text{m}} = 83$ °C), 1:1 ($T_{\text{m}} = 22$ °C), and 1:2 ratio (T_{m} : not reported) for G2–Li[TFSA] mixtures.^{28,29} In crystalline solvates with THF reported in the literature,^{30,31} Li⁺ ions are mostly solvated by four THF molecules (4-fold coordination) in the form of [Li(THF)₄]⁺ complex cations.

Whereas a favorable coordination number for Li⁺ ions is known to be 4–5 in solution,³² complexes with 6-fold coordination via the oxygen atoms of ether solvents, as observed in [Li(G1)₃][TFSA], [Li(G2)₂][TFSA], and [Li(G5)₁][TFSA], seem to be more stable in the crystalline state. Indeed, they generally possess a higher melting point than other solvates which exhibit 4- or 5-fold coordination. Because the solvates with 4- or 5-fold coordination possess low melting points, they are appropriate for the prime focus of this study. Table 1 summarizes the electrolyte properties (viscosity η , density ρ , molar concentration, and ionic conductivity σ) of [Li(glyme or THF)_x][TFSA] for which the ratio of Li⁺ ions and oxygen atoms of the solvent ([O]/[Li⁺]) is 4 or 5. [Li(THF)₄][TFSA], [Li(G1)₂][TFSA], and [Li(G2)_{4/3}][TFSA] possess the same [O]/[Li⁺] ratio as that of [Li(G3)₁][TFSA]. [Li(G1)_{5/2}][TFSA] can be considered an analogue of [Li(G4)₁][TFSA]. The density and molar concentration are in the order of [Li(G3)₁] > [Li(G2)_{4/3}] > [Li(G1)₂] > [Li(THF)₄], which is in accordance with the number of the oxygen atoms in each ligand molecule. [Li(G2)_{4/3}][TFSA] shows the lowest ionic conductivity, even with a comparable viscosity to that of [Li(G3)₁][TFSA].

In the reported single crystal structures of both [Li(THF)₄]-X^{30,31} and [Li(G1)₂]-X^{33,34} with different counteranions X, all of the oxygen atoms of the solvent bind to the Li⁺ ion to form the solvated cations [Li(THF)₄]⁺ and [Li(G1)₂]⁺. [Li(THF)₄]-[TFSA], and [Li(G1)₂][TFSA] would also possess a structurally similar complex cation to each analogue in their crystalline states, although the actual crystal structure is unknown for these solvates. As shown in Figure 3a and Table 1; however, the $D_{\text{sol}}/D_{\text{Li}}$ ratios are greater than 1 for the molten complexes [Li(THF)₄][TFSA] and [Li(G1)₂][TFSA], as well as the nonstoichiometric [Li(G1)_{5/2}][TFSA]. These results suggest that the complex cations are unstable in the melt, and

they possess either uncoordinated solvents or short-lived complex cations where ligand exchange takes place rapidly between the solvent and the anion in the liquid state. In this respect, the molten state of stable THF and G1 solvates such as $[\text{Li}(\text{THF})_4][\text{TFSA}]$ and $[\text{Li}(\text{G1})_2][\text{TFSA}]$ may not be classified as solvate ILs. The coordinating or weakly coordinating (highly exchangeable) solvents can screen the strong interaction between the ions, thereby reducing the viscosity even in dense electrolytes such as $[\text{Li}(\text{THF})_4][\text{TFSA}]$ and $[\text{Li}(\text{G1})_2][\text{TFSA}]$ (see Table 1).

For $[\text{Li}(\text{G2})_{4/3}][\text{TFSA}]$ (in which the mixed ratio is not stoichiometric to form the isolated solvates), the molten mixture of the stable complexes $[\text{Li}(\text{G2})_2][\text{TFSA}]$ and $[\text{Li}(\text{G2})_1][\text{TFSA}]$ may account for the almost equivalent diffusivity of the solvents and Li^+ ions. Because uncoordinated solvents with a long lifetime are scarcely present in the nonstoichiometric $[\text{Li}(\text{G2})_{4/3}][\text{TFSA}]$, this molten mixture can be regarded as a solvate IL. In the $[\text{Li}(\text{G2})_2][\text{TFSA}]$ crystal structure reported by Henderson et al.,²⁶ the Li^+ ion is six-coordinate (by the two G2 molecules), while the $[\text{TFSA}]^-$ counteranion remains uncoordinated in the form of a solvent separated ion pair (SSIP). The crystal structure of $[\text{Li}(\text{G2})_1][\text{TFSA}]$ was postulated based on the analogous single crystal structure $[\text{Li}(\text{G2})_1][\text{CF}_3\text{SO}_3]$ consisting of binuclear $[\text{Li}_2(\text{G2})_2]$ complexes cross-linked by the two anions; each five-coordinate Li^+ ion is coordinated by one G2 molecule and by two oxygen atoms from the two anions (one each from two anions).³⁵ This dimeric form may partially form in the liquid state and would be responsible for the lower ionic conductivity (Table 1) and diffusion coefficients of the components (Supporting Information Table S1) in $[\text{Li}(\text{G2})_{4/3}][\text{TFSA}]$, despite a comparable viscosity to that of $[\text{Li}(\text{G3})_1][\text{TFSA}]$.

From the $D_{\text{sol}}/D_{\text{Li}}$ results discussed above, $[\text{Li}(\text{glyme or THF})_x][\text{TFSA}]$ mixtures with an $[\text{O}]/[\text{Li}^+]$ ratio of 4 or 5 can be classified into two liquids: concentrated solutions or solvate ILs. $[\text{Li}(\text{THF})_4]^+$ and $[\text{Li}(\text{G1})_2]^+$ solvate cations were not adequately stable in their molten states, and thus $[\text{Li}(\text{THF})_4][\text{TFSA}]$ and $[\text{Li}(\text{G1})_2][\text{TFSA}]$ showed ordinal electrolyte solution behavior. In contrast, $[\text{Li}(\text{G3 or G4})_1]^+$ complex cations adopting crown ether-like coordination geometries are long-lived and behave like an independent cation in $[\text{Li}(\text{G3 or G4})_1][\text{TFSA}]$ solvate ILs.⁵ Judging by the thermal stability of $[\text{Li}(\text{G3 or G4})_1][\text{TFSA}]$ solvate ILs,^{4,5} there is no free glyme activity, and the lifetime of the solvates are long enough to call them solvate ILs. $[\text{Li}(\text{G2})_{4/3}][\text{TFSA}]$ behaved as a solvate IL although it is not an isolated solvate. It is suggested that solvate ionic liquids are formed when $\text{Li}[\text{TFSA}]$ is mixed with oligoethers possessing ethylene oxide units longer than G2 for the $[\text{Li}(\text{glyme})_x][\text{TFSA}]$ mixtures at an $[\text{O}]/[\text{Li}^+]$ ratio of 4 or 5.

Chelate Effect. It is clear that the $D_{\text{sol}}/D_{\text{Li}}$ ratio correlates to the lifetime of the $[\text{Li}(\text{glyme or THF})]^+$ complex cations in the liquid state. As shown in Figure 3, the longer glymes yield more robust complex cations with Li^+ , even at the same $[\text{O}]/[\text{Li}]$ ratio. In this part of the study we verified that the chelate effect is effective for $[\text{Li}(\text{glyme or THF})]^+$ complex cations in the concentrated liquid regime.

The complex formation constant K is an important parameter quantifying the chelate effect and the stability of complexes. Although there are no reports addressing these constants in concentrated $[\text{Li}(\text{glyme or THF})_x][\text{TFSA}]$ mixtures, some studies have reported K in dilute solutions. The K values for the systems involving lithium picrate (as a

spectroscopic probe of lithium salts) and the glymes or THF (as a ligand) in 1,4-dioxane solutions have been studied by Tsvetanov et al., and the K values were found to be 0.95, 2.1, 8.5, 17.0, and 24.5 M^{-1} for THF, G1, G2, G3, and G4, respectively.³⁶ Using fluorenyl lithium as another lithium salt probe, the K values of the glymes in 1,4-dioxane solutions were reported to be 0.055, 3.1, 130, and 240 M^{-1} for G1, G2, G3, and G4, respectively.^{37,38} The K likely depends on various factors such as the lithium salt probe used, the solvent, and the Li salt concentration. Nevertheless, the $D_{\text{sol}}/D_{\text{Li}}$ ratios in the concentrated regime and the K values studied in dilute solutions correlate well in terms of the number of oxygen atoms in the single ligands; significantly lower K values for THF and G1 may be the cause of the $D_{\text{sol}}/D_{\text{Li}}$ ratio higher than 1, indicating the lower stability of the solvated Li^+ ions. This is supported by the stabilization energies (ΔE_{form}) studied by computational methods; ΔE_{form} for the formation of $[\text{Li}(\text{glyme})_1]^+$ complexes with the glymes were in the same order: $\text{G4} > \text{G3} > \text{G2} > \text{G1}$.³⁹ Molecular dynamics (MD) simulations have also shown that the solvent residence time near Li^+ ions was more than 1 order of magnitude longer for pentaglyme (G5) than for bidentate G1 and monodentate ethylene carbonate (EC) in dilute $\text{Li}[\text{TFSA}]$ solutions.⁴⁰

In a previous study, we estimated the ligand exchange time (τ_b) between the $[\text{Li}(\text{G3 or G4})_1]^+$ complex and the free glymes in $[\text{Li}(\text{G3 or G4})_2][\text{TFSA}]$ mixtures from ^1H NMR spectra, where $[\text{Li}(\text{G3 or G4})_2][\text{TFSA}]$ were assumed to be 1:1 mixtures of $[\text{Li}(\text{G3 or G4})_1][\text{TFSA}]$ complexes and free glymes. The τ_b value can be estimated by the following equation in limited situations ($\tau_b \ll (2\pi\delta\nu)^{-1}$):⁴¹

$$\tau_b = \frac{2(W - W_0)}{\pi(\delta\nu)^2} \quad (2)$$

where W_0 and W are the full width at half-maximum (fwhm) of the NMR signals of the terminal glyme methoxy proton and $[\text{Li}(\text{G3 or G4})_2][\text{TFSA}]$, respectively. $\delta\nu$ is the difference in the chemical shift of the end methoxy proton of $[\text{Li}(\text{G3 or G4})_1][\text{TFSA}]$ and pure glyme. The τ_b value for the G3 or G4 systems are 1.9×10^{-4} and $3.6 \times 10^{-4} \text{ s}$, respectively.⁵ We applied the same procedure to the concentrated mixtures of the shorter glymes, and the NMR results are shown in Supporting Information Figure S2. However, the above equation may be invalid for $[\text{Li}(\text{G2})_{4/3}][\text{TFSA}]$ because of its nonstoichiometric composition. Furthermore, we encountered experimental difficulties in NMR measurements of $[\text{Li}(\text{G2})_x][\text{TFSA}]$ because the concentrated mixtures were prone to solidification at room temperature. For $[\text{Li}(\text{G1})_2][\text{TFSA}]$, τ_b can be approximated to a time scale of 10^{-5} – 10^{-6} s using the above equation, which is much shorter than those reported for $[\text{Li}(\text{G3 or G4})_1][\text{TFSA}]$. It is known that the water exchange time scale on Li^+ is extremely fast ($\tau_b \sim 10^{-9} \text{ s}$).⁴² Likewise, it can be assumed that τ_b for the mixtures with monodentate THF is even shorter than that for the mixtures with G1 although it is impossible to follow the exchange for THF on Li^+ by NMR. Thus, we can conclude the order of the lifetimes is $\text{G4} > \text{G3} \gg \text{G1} \gg \text{THF}$.

The different ion–solvent interactions based on the chelate effect would also be reflected in ion–ion interactions in concentrated mixtures, because there is competition between the solvent and $[\text{TFSA}]^-$ for the interaction with Li^+ ions. Figure 4 presents Raman spectra ranging from 730 to 760 cm^{-1} for $[\text{Li}(\text{glyme or THF})_x][\text{TFSA}]$ at an $[\text{O}]/[\text{Li}^+]$ ratio of 4.

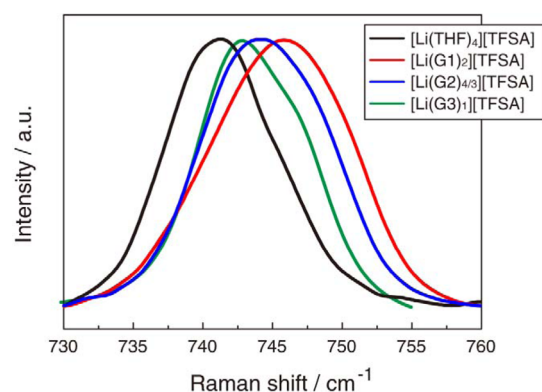


Figure 4. Raman spectra of $[\text{Li}(\text{glyme or THF})_x][\text{TFSA}]$ mixtures at an $[\text{O}]/[\text{Li}^+]$ ratio of 4.

The peaks at this frequency range have been assigned to the CF_3 bending vibration coupled with the S–N stretching vibration of $[\text{TFSA}]^-$ and is very sensitive to the $\text{Li}^+ - [\text{TFSA}]^-$ interaction.⁴³ The band corresponding to a SSIP or an uncoordinated $[\text{TFSA}]^-$ anion appears at $739\text{--}742\text{ cm}^{-1}$, whereas the band between 745 and 755 cm^{-1} originates from $[\text{TFSA}]^-$ bound directly to Li^+ ions in the form of a contact ion pair (CIP) or aggregate coordination (AGG).^{29,44} As shown in Figure 4, the peak shifted to higher frequency in the sequence $[\text{Li}(\text{THF})_4] < [\text{Li}(\text{G3})_1] < [\text{Li}(\text{G2})_{4/3}] < [\text{Li}(\text{G1})_2]$. Except for $[\text{Li}(\text{THF})_4][\text{TFSA}]$, this order correlates with the number of ethylene oxide units in the glyme, suggesting that the association of $[\text{TFSA}]^-$ with Li^+ ions is more predominant in $[\text{Li}(\text{G1})_2][\text{TFSA}]$ than in $[\text{Li}(\text{G3})_1][\text{TFSA}]$, even at the same $[\text{O}]/[\text{Li}^+]$ ratio. This is corroborated by weaker ion–solvent interactions for the shorter G1, as discussed in the studies on $D_{\text{sol}}/D_{\text{Li}}$ and K . The lowest peak frequency for $[\text{Li}(\text{THF})_4][\text{TFSA}]$ was probably due to its lower concentration (2.09 mol dm^{-3}) compared to the other mixtures ($\sim 3\text{ mol dm}^{-3}$). The steric hindrance of $[\text{Li}(\text{THF})_4]^+$ —being less crowded than the glyme-based complex cations when interacting with $[\text{TFSA}]^-$ —was also reflected by the lowest peak frequency. When the Raman spectra were compared at commensurate concentrations of $\sim 3\text{ mol dm}^{-3}$, the peak shifted to higher frequency with decreasing number of oxygen atoms in the solvent: $[\text{Li}(\text{G3})_1] < [\text{Li}(\text{G2})_{4/3}] < [\text{Li}(\text{G1})_2] < [\text{Li}(\text{THF})_2]$ (see Supporting Information Table S1 and Figure S3).

Chelate Effect on Physicochemical Properties. In this section, we demonstrate how the stability of the complex cation arising from the chelate effect correlates with the properties of the concentrated $[\text{Li}(\text{glyme or THF})_x][\text{TFSA}]$ mixtures. Generally, solvate ILs should possess high thermal stability—as is typical for ILs—owing to the strong complexation between Li^+ ions and the ligands. The thermal decomposition temperature (T_d) and its difference (ΔT_d) from T_d of the pure solvents of the $[\text{Li}(\text{glyme or THF})_x][\text{TFSA}]$ mixtures at $[\text{O}]/[\text{Li}^+]$ ratio of 4 or 5 were studied by thermogravimetric analysis (Supporting Information Figure S4) and are shown in Figure 5. It is apparent that the relatively low T_d and ΔT_d values for $[\text{Li}(\text{THF})_x][\text{TFSA}]$ and $[\text{Li}(\text{G1})_x][\text{TFSA}]$ —which are not solvate ILs—are attributed to the high volatility of the uncoordinated or weakly interacting solvents found in these solution-like mixtures. However, for the other mixtures exhibiting $D_{\text{sol}}/D_{\text{Li}} \sim 1$, ΔT_d is more pronounced, and the thermal stability is dramatically improved by the strong complexation between Li^+ ions and the longer glymes such as

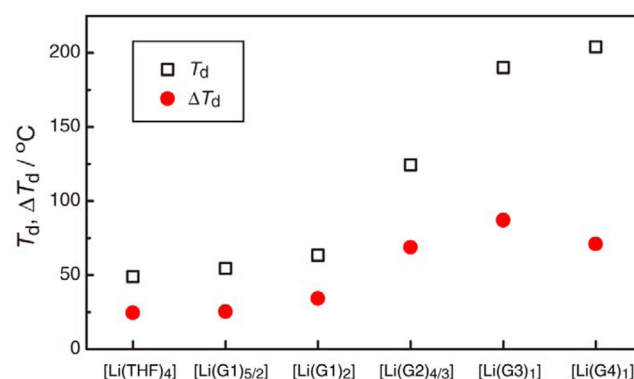


Figure 5. Thermal decomposition temperature (T_d) and its difference (ΔT_d) from T_d of the pure solvents of $[\text{Li}(\text{glyme or THF})_x][\text{TFSA}]$ mixtures.

G2, G3, and G4, yielding solvate ILs. The ΔT_d of $[\text{Li}(\text{G3})_1][\text{TFSA}]$ ($[\text{O}]/[\text{Li}^+] = 4$) was slightly higher than that of $[\text{Li}(\text{G4})_1][\text{TFSA}]$ ($[\text{O}]/[\text{Li}^+] = 5$), implying that the coordination number of 4 offers the most thermally stable conditions.

Figure 6 illustrates linear sweep voltammograms at a Pt electrode for the $[\text{Li}(\text{glyme or THF})_x][\text{TFSA}]$ concentrated

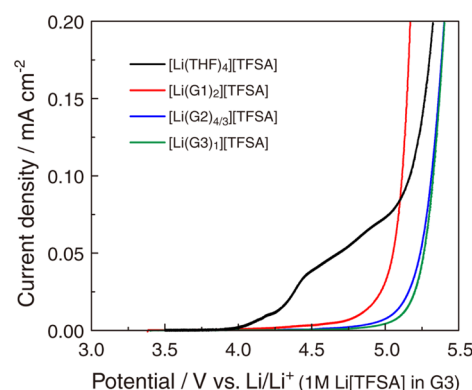


Figure 6. Linear sweep voltammograms of $[\text{Li}(\text{glyme or THF})_x][\text{TFSA}]$ at scan rate 1 mV s^{-1} at $30\text{ }^\circ\text{C}$.

mixtures. Interestingly, almost no current is detected below 4.5 V vs Li/Li^+ for the solvate ILs $[\text{Li}(\text{G2})_{4/3}][\text{TFSA}]$ and $[\text{Li}(\text{G3})_1][\text{TFSA}]$, whereas obvious current flow can be seen at potentials higher than 4 V vs Li/Li^+ for $[\text{Li}(\text{THF})_4][\text{TFSA}]$ and $[\text{Li}(\text{G1})_2][\text{TFSA}]$. The ether solvents oxidatively decomposed at lower potentials in the solution-like $[\text{Li}(\text{THF})_4][\text{TFSA}]$ and $[\text{Li}(\text{G1})_2][\text{TFSA}]$. However, the formation of the stable complex cation in the lithium solvate ILs $[\text{Li}(\text{G2})_{4/3}][\text{TFSA}]$ and $[\text{Li}(\text{G3})_1][\text{TFSA}]$ lowers the HOMO energy level of the oligoether solvents and thus effectively suppresses the oxidative decomposition.⁵

The properties of $[\text{Li}(\text{G2})_{4/3}][\text{TFSA}]$ and $[\text{Li}(\text{G3 or G4})_1][\text{TFSA}]$ discussed above are all ascribed to the formation of stable complex cations. Therefore, the present lithium solvate ILs have many desirable properties such as high thermal and electrochemical stability, and high Li^+ concentration; they are therefore promising electrolytes for not only lithium ion batteries but also high-energy density batteries such as lithium–sulfur and lithium–air batteries.

Ionicity. The effect of the stability of complex cations on the dynamics of ionic transport is also of interest. Ionicity—also

known as the molar conductivity ratio ($\Lambda_{\text{imp}}/\Lambda_{\text{NMR}}$)—has been used to estimate the degree of dissociation of lithium salts in dilute electrolytes²¹ and can also be a useful metric for quantifying the dissociativity or degree of correlative motion of ions, even in extremely concentrated systems such as ILs.^{45,46}

Λ_{imp} is the molar conductivity measured by the AC impedance method, while Λ_{NMR} can be calculated from the ionic self-diffusion coefficients D_{Li} and D_{TFSA} (measured by PGSE NMR) using the Nernst–Einstein equation:

$$\Lambda_{\text{NMR}} = \frac{F^2}{RT} (D_{\text{Li}} + D_{\text{TFSA}}) \quad (3)$$

where F is the Faraday constant, R is the gas constant, and T is the absolute temperature. This equation postulates that all diffusing species detected by PGSE NMR contribute to the molar conductivity. In contrast, Λ_{imp} relies on the net migration of charged species in an electric field. Therefore, the ratio $\Lambda_{\text{imp}}/\Lambda_{\text{NMR}}$ accounts for the proportion of ions (charged species) that participate in ionic conduction from all diffusing species on the measurement time scale, enabling diagnosis of the correlation of ionic motion affected by ionic interactions.^{47,48} $\Lambda_{\text{imp}}/\Lambda_{\text{NMR}}$ is often represented as $\Lambda/\Lambda_{\text{NE}}$ in the literature⁴⁹ and is reciprocal of the well-known Haven ratio.^{50,51}

In a previous study, we found that the ratio $\Lambda_{\text{imp}}/\Lambda_{\text{NMR}}$ exhibited its highest value at a 1:1 equimolar composition of $[\text{Li}(\text{G3 or G4})_x][\text{TFSA}]$ mixtures, which then decreased monotonically upon dilution. This phenomenon is opposite to that found in typical organic electrolytes—such as $\text{Li}[\text{TFSA}]$ in propylene carbonate (PC)—in which the ionicity increased with decreasing salt concentration, as predicted by classical electrolyte theories.^{52,53} In this section, we reexamine our findings for various oligoether-based mixtures—including shorter glymes and THF—over a wide range of $\text{Li}[\text{TFSA}]$ concentrations. Figures 7 and 8 show the ionicity of the

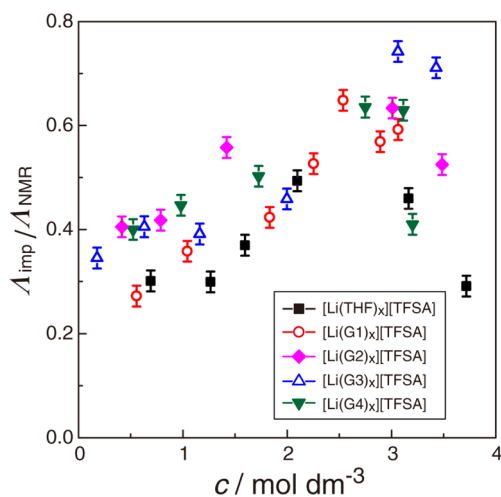


Figure 7. Ionicity ($\Lambda_{\text{imp}}/\Lambda_{\text{NMR}}$) at 30 °C for $[\text{Li}(\text{glyme or THF})_x][\text{TFSA}]$ mixtures as a function of concentration.

$[\text{Li}(\text{glyme or THF})_x][\text{TFSA}]$ mixtures as functions of concentration and the $[\text{O}]/[\text{Li}^+]$ ratio, respectively. Compared with other solvents (Figure 7), $[\text{Li}(\text{THF})_x][\text{TFSA}]$ mixtures tend to show lower ionicity, explaining the lower ionic conductivities of $[\text{Li}(\text{THF})_x][\text{TFSA}]$ than those of $[\text{Li}(\text{G1})_x][\text{TFSA}]$ (Figure 1). Similarly to the results previously reported for $[\text{Li}(\text{G3 or G4})_x][\text{TFSA}]$, $\Lambda_{\text{imp}}/\Lambda_{\text{NMR}}$ of $[\text{Li}(\text{G1, G2 or$

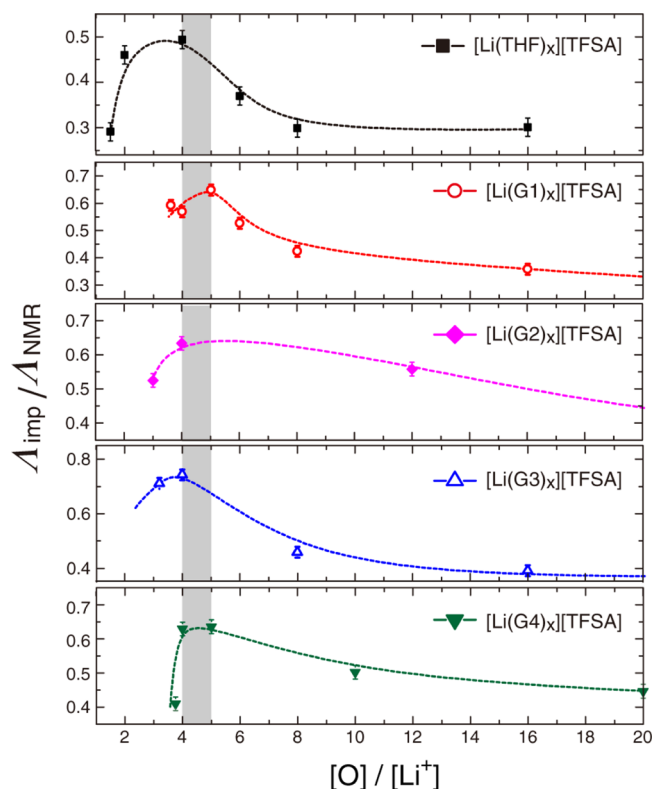


Figure 8. Ionicity ($\Lambda_{\text{imp}}/\Lambda_{\text{NMR}}$) at 30 °C for $[\text{Li}(\text{glyme or THF})_x][\text{TFSA}]$ mixtures as a function of $[\text{O}]/[\text{Li}^+]$ ratio. Lines are a guide to the eye.

$\text{THF})_x][\text{TFSA}]$ became lower upon dilution when the concentration was lower than 3 mol dm^{-3} . More noteworthy is that the ionicity reached a maximum in the concentration range of 2–3.1 mol dm^{-3} , before decreasing again at higher concentrations (>3 mol dm^{-3}) for all $[\text{Li}(\text{glyme or THF})_x][\text{TFSA}]$ mixtures. It was established for the first time in this study that the maximum ionicity occurs at an $[\text{O}]/[\text{Li}^+]$ ratio of 4 or 5 (Figure 8). Although we do not have a clear rationale for this behavior, it should be noted that the $[\text{O}]/[\text{Li}^+]$ ratio for the maximum ionicity agrees well with the favorable coordination number for Li^+ ions in the electrolyte. These results suggest that most uncorrelated cation–anion motions can be accomplished by the addition of a minimal amount of ether solvents that construct the first solvation shell of Li^+ ions (i.e., $[\text{O}]/[\text{Li}^+] \sim 4$ or 5).

The decrease in the ionicity upon dilution is likely common for ether-based $[\text{Li}(\text{glyme or THF})_x][\text{TFSA}]$ mixtures and independent of the number of oxygen atoms in the molecules. This is reminiscent of our previous results found in aprotic ILs with the addition of solvents with relatively low polarity.^{54,55} It was assumed that self-dissociable IL cations and anions form a relatively long-lived aggregate when diluted with low-polar solvents; cation–anion attractive forces would be enhanced in the presence of low-polarity solvents, rather than in neat ILs with well-balanced ionic interactions. Given the maximum ionicity results from an $[\text{O}]/[\text{Li}^+]$ ratio of ~ 4 or 5, these ratios may be sufficient for the dissociation of the solvated Li^+ and $[\text{TFSA}]^-$. In a fashion similar to the mixtures of aprotic ILs and low-polarity solvents, further addition of glymes or THF with low permittivity ($\epsilon = 7\text{--}8$)⁵⁶ may bring about ionic association, where the excess solvent would serve as a low dielectric medium. Raman spectra of $[\text{TFSA}]^-$ in $[\text{Li}(\text{glyme or$

THF)_x][TFSA] (Supporting Information Figure S3) indicate that the number of either uncoordinated or SSIP-type [TFSA][−] species increased upon dilution. Therefore, Raman spectra and the lowered ionicity would suggest that loosely bound ion pairs (or ionic aggregates) composed of solvated cations and [TFSA] (i.e., SSIPs) are formed in dilute [Li(glyme or THF)_x][TFSA] mixtures.

Such behavior is common for the oligoethers studied in this work. However, this is probably not the case for other nonaqueous aprotic solvents with higher permittivity—such as PC ($\epsilon \sim 64$)—where Coulombic attractions between the solvated cation and the counteranions are more shielded.^{57,58} In MD simulations by Borodin and Smith, a noticeable dynamic correlation of ionic motion was found in dilute Li[TFSA] solutions in less polar G1, while completely uncorrelated Li⁺ and [TFSA][−] motion was observed in dilute Li[TFSA] solutions in polar EC.^{40,59}

The decrease in the ionicity at an [O]/[Li⁺] ratio lower than 4 (highly concentrated regime) is probably due to the strong association of Li⁺ with [TFSA][−]. In these extremely concentrated conditions, [TFSA][−] must participate in the solvation of Li⁺ to satisfy the lowest coordination number of 4 for Li⁺ ions. This gives rise to a long-lived CIP or AGG, as evidenced by the Raman band of [TFSA][−] in the range of 730–760 cm^{−1} further shifting to high frequency at an [O]/[Li⁺] ratio less than 4 (see Supporting Information Figure S3). Hence, Li⁺ and [TFSA][−] migrate collectively in the form of a CIP and/or AGG, leading to a drastic decrease in the ionicity.

Therefore, the ligands (the solvent or the anion) in the first coordination sphere of Li⁺ ions are responsible for the ionicity value in highly concentrated regimes, whereas the dipolar properties of the solvent dominate the ionicity in dilute regimes.

4. CONCLUSION

In this study, the effect of the solvent nature on the properties of [Li(glyme or THF)_x][TFSA] mixtures were studied over a wide range of Li[TFSA] concentrations. In concentrated regions where the [O]/[Li⁺] ratio was adjusted to be 4 or 5, the mixtures yielding the solvate ILs could be distinguished from the concentrated solutions by analyzing the self-diffusion coefficient ratio $D_{\text{sol}}/D_{\text{Li}}$; the ratio was always greater than 1 in concentrated solutions ([Li(G1 or THF)_x][TFSA] mixtures) even when the molar concentration was higher than 3 mol dm^{−3}, whereas the solvate ILs ([Li(G3 or G4)₁][TFSA] and [Li(G2)_{4/3}][TFSA]) showed a $D_{\text{sol}}/D_{\text{Li}}$ of ~ 1 , indicating long-lived complex cations. The chelate effect explained differences in the stability of the complex cations among [Li(glyme or THF)_x][TFSA] mixtures with an [O]/[Li⁺] ratio of ~ 4 or 5. The stable solvate cations could be formed with longer glymes and afforded high thermal and electrochemical stability. The solvate ILs [Li(G3)₁][TFSA] and [Li(G2)_{4/3}][TFSA] significantly suppressed oxidative decomposition, whereas notable decomposition occurred in concentrated [Li(THF)₄][TFSA] and [Li(G1)₂][TFSA] solutions at lower potentials. The maximum ionicity ($\Lambda_{\text{imp}}/\Lambda_{\text{NMR}}$) of [Li(glyme or THF)_x][TFSA] mixtures was found at a concentration range of [O]/[Li⁺] ~ 4 or 5, and the ionicity decreased both in the higher and lower concentration ranges. To understand this ionicity behavior, two solvent effects were considered: the solvating effect of the ligands (the solvent and/or the anion) in the first coordination shell for the concentrated regime, and the dipolar effect of the solvent in the dilute regime. This study revealed

the importance of ion–dipole (ion-induced dipole) interactions and the chelate effect in the behavior of solvate ILs as distinguished from concentrated electrolyte solutions.

■ ASSOCIATED CONTENT

Supporting Information

Figures showing DSC thermograms for [Li(G3)₁][TFSA] and [Li(G5)₁][TFSA], ¹H NMR spectra of [Li(G1)_x][TFSA], Raman spectra of [Li(THF)_x][TFSA] and [Li(G4)_x][TFSA] as a function of lithium concentration, and thermogravimetric curves for [Li(glyme or THF)_x][TFSA] and a table listing electrolyte properties of [Li(glyme or THF)_x][TFSA] mixtures. This material is available free of charge via the Internet at <http://pubs.acs.org>.

■ AUTHOR INFORMATION

Corresponding Author

*Tel./Fax: +81-45-339-3955. E-mail: mwatanab@ynu.ac.jp.

Author Contributions

[§]C.Z. and K.U. contributed equally to this work.

Notes

The authors declare no competing financial interest.

■ ACKNOWLEDGMENTS

This study was supported in part by the Advanced Low Carbon Technology Research and Development Program (ALCA) of the Japan Science and Technology Agency (JST) and by the Technology Research Grant Program of the New Energy and Industrial Technology Development Organization (NEDO) of Japan. C.Z. thanks the China Scholarship Council (CSC) for financial support.

■ REFERENCES

- (1) Angell, C. A. A New Class of Molten Salt Mixtures The Hydrated Dipositive Ion as an Independent Cation Species. *J. Electrochem. Soc.* **1965**, *112* (12), 1224–1227.
- (2) Angell, C. A.; Ansari, Y.; Zhao, Z. Ionic Liquids: Past, present and future. *Faraday Discuss.* **2012**, *154*, 9–27.
- (3) Tamura, T.; Hachida, T.; Yoshida, K.; Tachikawa, N.; Dokko, K.; Watanabe, M. New glyme-cyclic imide lithium salt complexes as thermally stable electrolytes for lithium batteries. *J. Power Sources* **2010**, *195* (18), 6095–6100.
- (4) Tamura, T.; Yoshida, K.; Hachida, T.; Tsuchiya, M.; Nakamura, M.; Kazue, Y.; Tachikawa, N.; Dokko, K.; Watanabe, M. Physicochemical Properties of Glyme–Li Salt Complexes as a New Family of Room-temperature Ionic Liquids. *Chem. Lett.* **2010**, *39* (7), 753–755.
- (5) Yoshida, K.; Nakamura, M.; Kazue, Y.; Tachikawa, N.; Tsuzuki, S.; Seki, S.; Dokko, K.; Watanabe, M. Oxidative-Stability Enhancement and Charge Transport Mechanism in Glyme–Lithium Salt Equimolar Complexes. *J. Am. Chem. Soc.* **2011**, *133* (33), 13121–13129.
- (6) Yoshida, K.; Tsuchiya, M.; Tachikawa, N.; Dokko, K.; Watanabe, M. Correlation between Battery Performance and Lithium Ion Diffusion in Glyme–Lithium Bis(trifluoromethanesulfonyl)amide Equimolar Complexes. *J. Electrochem. Soc.* **2012**, *159* (7), A1005–A1012.
- (7) Seki, S.; Takei, K.; Miyashiro, H.; Watanabe, M. Physicochemical and Electrochemical Properties of Glyme–LiN(SO₂F)₂ Complex for Safe Lithium-ion Secondary Battery Electrolyte. *J. Electrochem. Soc.* **2011**, *158* (6), A769–A774.
- (8) Orita, A.; Kamijima, K.; Yoshida, M.; Dokko, K.; Watanabe, M. Favorable combination of positive and negative electrode materials with glyme–Li salt complex electrolytes in lithium ion batteries. *J. Power Sources* **2011**, *196* (8), 3874–3880.

- (9) Tachikawa, N.; Yamauchi, K.; Takashima, E.; Park, J.-W.; Dokko, K.; Watanabe, M. Reversibility of electrochemical reactions of sulfur supported on inverse opal carbon in glyme-Li salt molten complex electrolytes. *Chem. Commun. (Cambridge, U. K.)* **2011**, 47 (28), 8157–8159.
- (10) Dokko, K.; Tachikawa, N.; Yamauchi, K.; Tsuchiya, M.; Yamazaki, A.; Takashima, E.; Park, J.-W.; Ueno, K.; Seki, S.; Serizawa, N.; Watanabe, M. Solvate Ionic Liquid Electrolyte for Li–S Batteries. *J. Electrochem. Soc.* **2013**, 160 (8), A1304–A1310.
- (11) Ueno, K.; Park, J.-W.; Yamazaki, A.; Mandai, T.; Tachikawa, N.; Dokko, K.; Watanabe, M. Anionic Effects on Solvate Ionic Liquid Electrolytes in Rechargeable Lithium–Sulfur Batteries. *J. Phys. Chem. C* **2013**, 117 (40), 20509–20516.
- (12) McOwen, D. W.; Seo, D. M.; Borodin, O.; Vatamanu, J.; Boyle, P. D.; Henderson, W. A. Concentrated electrolytes: Decrypting electrolyte properties and reassessing Al corrosion mechanisms. *Energy Environ. Sci.* **2014**, 7 (1), 416–426.
- (13) Suo, L.; Hu, Y.-S.; Li, H.; Armand, M.; Chen, L. A New Class of Solvent-in-Salt Electrolyte for High-Energy Rechargeable Metallic Lithium Batteries. *Nat. Commun.* **2013**, 4, 1481.
- (14) Shin, E. S.; Kim, K.; Oh, S. H.; Cho, W. I. Polysulfide Dissolution Control: The Common Ion Effect. *Chem. Commun. (Cambridge, U. K.)* **2013**, 49, 2004–2006.
- (15) Ueno, K.; Yoshida, K.; Tsuchiya, M.; Tachikawa, N.; Dokko, K.; Watanabe, M. Glyme–Lithium Salt Equimolar Molten Mixtures: Concentrated Solutions or Solvate Ionic Liquids? *J. Phys. Chem. B* **2012**, 116 (36), 11323–11331.
- (16) Part II of this study deals with the importance of solvate-structure stability for electrolytes of Li-ion Li-S batteries. *J. Phys. Chem. B* **2014**, submitted for publication.
- (17) Tokuda, H.; Hayamizu, K.; Ishii, K.; Abu Bin Hasan Susan, Md.; Watanabe, M. Physicochemical properties and structures of room temperature ionic liquids. 1. Variation of anionic species. *J. Phys. Chem. B* **2004**, 108 (42), 16593–16600.
- (18) Price, W. S. *NMR Studies of Translational Motion: Principles and Applications*; Cambridge University Press: Cambridge, U.K., 2009.
- (19) Yoshida, K.; Tsuchiya, M.; Tachikawa, N.; Dokko, K.; Watanabe, M. Change from Glyme Solutions to Quasi-ionic Liquids for Binary Mixtures Consisting of Lithium Bis-(trifluoromethanesulfonyl)amide and Glymes. *J. Phys. Chem. C* **2011**, 115 (37), 18384–18394.
- (20) Brouillette, D.; Perron, G.; Desnoyers, J. E. Apparent molar volume, heat capacity, and conductance of lithium bis-(trifluoromethylsulfone)imide in glymes and other aprotic solvents. *J. Solution Chem.* **1998**, 27 (2), 151–182.
- (21) Hayamizu, K.; Aihara, Y.; Arai, S.; Martinez, C. G. Pulse-gradient spin-echo ^1H , ^7Li , and ^{19}F NMR diffusion and ionic conductivity measurements of 14 organic electrolytes containing $\text{LiN}(\text{SO}_2\text{CF}_3)_2$. *J. Phys. Chem. B* **1999**, 103 (3), 519–524.
- (22) Hayamizu, K.; Akiba, E.; Bando, T.; Aihara, Y. ^1H , ^7Li , and ^{19}F nuclear magnetic resonance and ionic conductivity studies for liquid electrolytes composed of glymes and polyethyleneglycol dimethyl ethers of $\text{CH}_3\text{O}(\text{CH}_2\text{CH}_2\text{O})_n\text{CH}_3$ ($n=3\text{--}50$) doped with $\text{LiN}(\text{SO}_2\text{CF}_3)_2$. *J. Chem. Phys.* **2002**, 117 (12), 5929–5939.
- (23) Tokuda, H.; Hayamizu, K.; Ishii, K.; Susan, M.; Watanabe, M. Physicochemical properties and structures of room temperature ionic liquids. 2. Variation of alkyl chain length in imidazolium cation. *J. Phys. Chem. B* **2005**, 109 (13), 6103–6110.
- (24) Henderson, W. A.; Brooks, N. R.; Brennessel, W. W.; Young, V. G. Triglyme-Li⁺ cation solvate structures: Models for amorphous concentrated liquid and polymer electrolytes (I). *Chem. Mater.* **2003**, 15 (24), 4679–4684.
- (25) Henderson, W. A.; Brooks, N. R.; Young, V. G. Tetraglyme-Li⁺ cation solvate structures: Models for amorphous concentrated liquid and polymer electrolytes (II). *Chem. Mater.* **2003**, 15 (24), 4685–4690.
- (26) Henderson, W. A.; McKenna, F.; Khan, M. A.; Brooks, N. R.; Young, V. G.; Frech, R. Glyme–Lithium Bis-(trifluoromethanesulfonyl)imide and Glyme–Lithium Bis-(perfluoroethanesulfonyl)imide Phase Behavior and Solvate Structures. *Chem. Mater.* **2005**, 17 (9), 2284–2289.
- (27) Lascaud, S.; Perrier, M.; Vallee, A.; Besner, S.; Prud'homme, J.; Armand, M. Phase Diagrams and Conductivity Behavior of Poly-(ethylene oxide)-Molten Salt Rubbery Electrolytes. *Macromolecules* **1994**, 27 (25), 7469–7477.
- (28) Henderson, W. A. Glyme–lithium salt phase behavior. *J. Phys. Chem. B* **2006**, 110 (26), 13177–13183.
- (29) Brouillette, D.; Irish, D. E.; Taylor, N. J.; Perron, G.; Odziemkowski, M.; Desnoyers, J. E. Stable solvates in solution of lithium bis(trifluoromethylsulfone)imide in glymes and other aprotic solvents: Phase diagrams, crystallography and Raman spectroscopy. *Phys. Chem. Chem. Phys.* **2002**, 4 (24), 6063–6071.
- (30) Serrano, C. B.; Less, R. J.; McPartlin, M.; Naseri, V.; Wright, D. S. The First-Row Transition Metal Interstitial Hydride Anion $[\{\text{PhP}(\text{CH}_2)_3\text{Fe}\}_4(\mu_4\text{H})]^-$. *Organometallics* **2010**, 29 (22), 5754–5756.
- (31) Sazama, G. T.; Betley, T. A. Ligand-Centered Redox Activity: Redox Properties of 3d Transition Metal Ions Ligated by the Weak-Field Tris(pyrrolyl)ethane Trianion. *Inorg. Chem.* **2010**, 49 (5), 2512–2524.
- (32) Kameda, Y.; Umabayashi, Y.; Takeuchi, M.; Wahab, M. A.; Fukuda, S.; Ishiguro, S.; Sasaki, M.; Amo, Y.; Usuki, T. Solvation Structure of Li^+ in Concentrated LiPF_6 –Propylene Carbonate Solutions. *J. Phys. Chem. B* **2007**, 111 (22), 6104–6109.
- (33) Becker, G.; Eschbach, B.; Mundt, O.; Reti, M.; Niecke, E.; Issberner, K.; Nieger, M.; Thelen, V.; Nöth, H.; Waldhör, R.; Schmidt, M. Bis(1,2-dimethoxyethan-O,O')lithium-phosphanid, -arsanid und -chlorid—drei neue Vertreter des Bis(1,2-dimethoxyethan-O,O')-lithium-bromid-Typs. *Z. Anorg. Allg. Chem.* **1998**, 624 (3), 469–482.
- (34) Henderson, W. A.; Brooks, N. R.; Brennessel, W. W.; Young, V. G. LiClO_4 Electrolyte Solvate Structures. *J. Phys. Chem. A* **2003**, 108 (1), 225–229.
- (35) Rhodes, C. P.; Frech, R. Local Structures in Crystalline and Amorphous Phases of Diglyme– LiCF_3SO_3 and Poly(ethylene oxide)– LiCF_3SO_3 Systems: Implications for the Mechanism of Ionic Transport. *Macromolecules* **2001**, 34 (8), 2660–2666.
- (36) Tsvetanov, C. B.; Petrova, E. B.; Dimov, D. K.; Panayotov, I. M.; Smid, J. Interactions of ligands with lithium picrate in dioxane. *J. Solution Chem.* **1990**, 19 (5), 425–436.
- (37) Chan, L.-L.; Smid, J. Contact and solvent-separated ion pairs of carbanions. IV. Specific solvation of alkali ions by polyglycol dimethyl ethers. *J. Am. Chem. Soc.* **1967**, 89 (17), 4547–4549.
- (38) Chan, L. L.; Wong, K. H.; Smid, J. Complexation of lithium, sodium, and potassium carbanion pairs with polyglycol dimethyl ethers (glymes). Effect of chain length and temperature. *J. Am. Chem. Soc.* **1970**, 92 (7), 1955–1963.
- (39) Tsuzuki, S.; Shinoda, W.; Seki, S.; Umabayashi, Y.; Yoshida, K.; Dokko, K.; Watanabe, M. Intermolecular Interactions in Li^+ -glyme and Li^+ -glyme–TFSA[−] Complexes: Relationship with Physicochemical Properties of $[\text{Li}(\text{glyme})][\text{TFSA}]$ Ionic Liquids. *ChemPhysChem* **2013**, 14 (9), 1993–2001.
- (40) Borodin, O.; Smith, G. D. Li⁺ Transport Mechanism in Oligo(Ethylene Oxide)s Compared to Carbonates. *J. Solution Chem.* **2007**, 36 (6), 803–813.
- (41) Allerhand, A.; Gutowsky, H. S.; Jonas, J.; Meinzer, R. A. Nuclear Magnetic Resonance Methods for Determining Chemical-Exchange Rates. *J. Am. Chem. Soc.* **1966**, 88 (14), 3185–3194.
- (42) Helm, L.; Merbach, A. E. Inorganic and Bioinorganic Solvent Exchange Mechanisms. *Chem. Rev.* **2005**, 105 (6), 1923–1960.
- (43) Umabayashi, Y.; Mitsugi, T.; Fukuda, S.; Fujimori, T.; Fujii, K.; Kanzaki, R.; Takeuchi, M.; Ishiguro, S.-I. Lithium Ion Solvation in Room-Temperature Ionic Liquids Involving Bis-(trifluoromethanesulfonyl) Imide Anion Studied by Raman Spectroscopy and DFT Calculations. *J. Phys. Chem. B* **2007**, 111 (45), 13028–13032.
- (44) Seo, D. M.; Borodin, O.; Han, S.-D.; Boyle, P. D.; Henderson, W. A. Electrolyte Solvation and Ionic Association II. Acetonitrile-

Lithium Salt Mixtures: Highly Dissociated Salts. *J. Electrochem. Soc.* **2012**, *159* (9), A1489–A1500.

(45) Tokuda, H.; Tsuzuki, S.; Susan, M.; Hayamizu, K.; Watanabe, M. How ionic are room-temperature ionic liquids? An indicator of the physicochemical properties. *J. Phys. Chem. B* **2006**, *110* (39), 19593–19600.

(46) Ueno, K.; Tokuda, H.; Watanabe, M. Ionicity in ionic liquids: Correlation with ionic structure and physicochemical properties. *Phys. Chem. Chem. Phys.* **2010**, *12* (8), 1649–1658.

(47) Harris, K. R. Relations between the Fractional Stokes–Einstein and Nernst–Einstein Equations and Velocity Correlation Coefficients in Ionic Liquids and Molten Salts. *J. Phys. Chem. B* **2010**, *114* (29), 9572–9577.

(48) Kashyap, H. K.; Annapureddy, H. V. R.; Raineri, F. O.; Margulis, C. J. How Is Charge Transport Different in Ionic Liquids and Electrolyte Solutions? *J. Phys. Chem. B* **2011**, *115* (45), 13212–13221.

(49) MacFarlane, D. R.; Forsyth, M.; Izgorodina, E. I.; Abbott, A. P.; Annat, G.; Fraser, K. On the Concept of Ionicity in Ionic Liquids. *Phys. Chem. Chem. Phys.* **2009**, *11* (25), 4962–4967.

(50) Murch, G. E. The Haven Ratio in Fast Ionic Conductors. *Solid State Ionics* **1982**, *7* (3), 177–198.

(51) Fromling, T.; Kunze, M.; Schonhoff, M.; Sundermeyer, J.; Roling, B. Enhanced Lithium Transference Numbers in Ionic Liquid Electrolytes. *J. Phys. Chem. B* **2008**, *112* (41), 12985–12990.

(52) Robinson, R. A.; Stokes, R. H. *Electrolyte Solutions*; Dover Publications: Mineola, NY, USA, 1970.

(53) Bockris, J. O. M.; Reddy, A. K. N. *Modern Electrochemistry 1: Ionics*; Springer: Berlin, Germany, Berlin, Germany, 1998.

(54) Tokuda, H.; Baek, S. J.; Watanabe, M. Room-temperature ionic liquid-organic solvent mixtures: Conductivity and ionic association. *Electrochemistry* **2005**, *73* (8), 620–622.

(55) Borodin, O.; Henderson, W. A.; Fox, E. T.; Berman, M.; Gobet, M.; Greenbaum, S. Influence of Solvent on Ion Aggregation and Transport in PY15TFSI Ionic Liquid–Aprotic Solvent Mixtures. *J. Phys. Chem. B* **2013**, *117* (36), 10581–10588.

(56) Choquette, Y.; Brisard, G.; Parent, M.; Brouillette, D.; Perron, G.; Desnoyers, J. E.; Armand, M.; Gravel, D.; Slougui, N. Sulfamides and Glymes as Aprotic Solvents for Lithium Batteries. *J. Electrochem. Soc.* **1998**, *145* (10), 3500–3507.

(57) Aihara, Y.; Sugimoto, K.; Price, W. S.; Hayamizu, K. Ionic conduction and self-diffusion near infinitesimal concentration in lithium salt-organic solvent electrolytes. *J. Chem. Phys.* **2000**, *113* (5), 1981–1991.

(58) Takeuchi, M.; Kameda, Y.; Umebayashi, Y.; Ogawa, S.; Sonoda, T.; Ishiguro, S.-i.; Fujita, M.; Sano, M. Ion–ion interactions of LiPF₆ and LiBF₄ in propylene carbonate solutions. *J. Mol. Liq.* **2009**, *148* (2–3), 99–108.

(59) Borodin, O.; Smith, G. D. LiTFSI Structure and Transport in Ethylene Carbonate from Molecular Dynamics Simulations. *J. Phys. Chem. B* **2006**, *110* (10), 4971–4977.